Inelastic diffraction with CMS

ISCRA-2021

Lev Kheyn

On Behalf of the CMS Collaboration

SINP MSU

Physics relevance

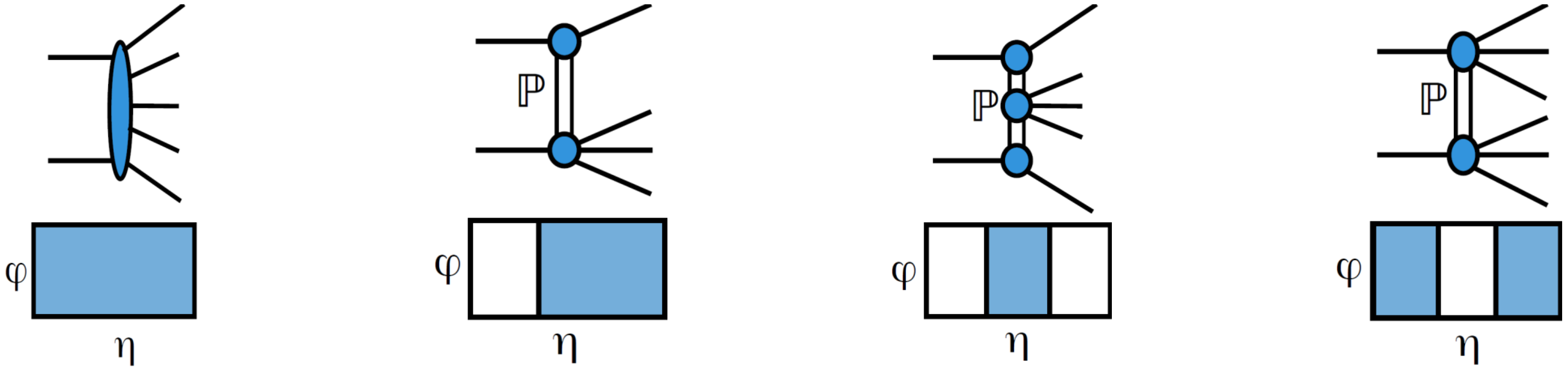

Non-Diffractive | Single Diffraction | Central Diffraction | Double Diffraction

- Most important problems of QCD which can be studied with diffraction:
  - Nature of the pomeron
  - Small-x & saturation
- Inelastic screening and/or non-linear effects (saturation) are enlarged in collisions with nuclei
- Inelastic diffraction largely contributes to uncertainty of air shower modeling

Inside CMS

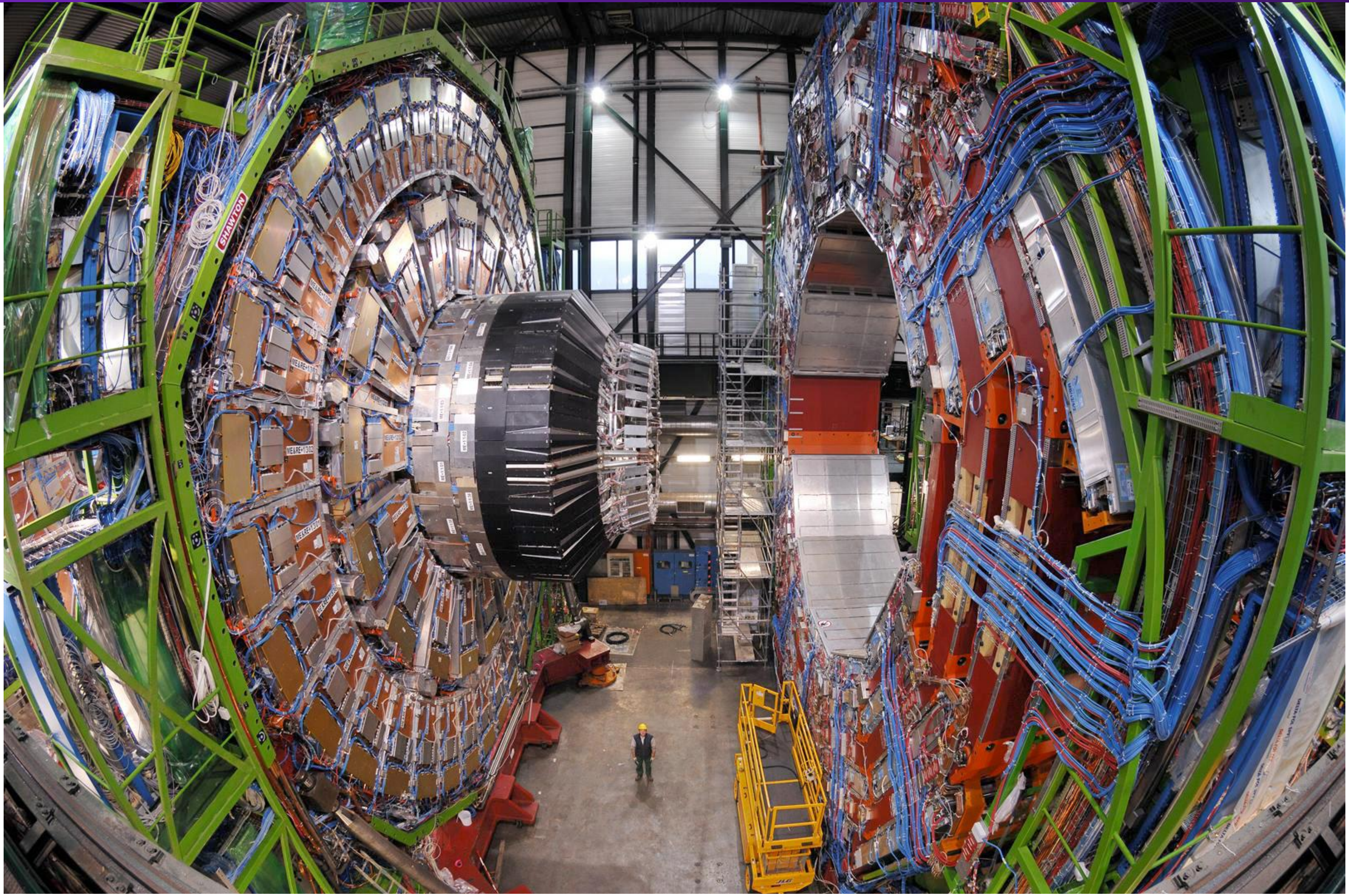

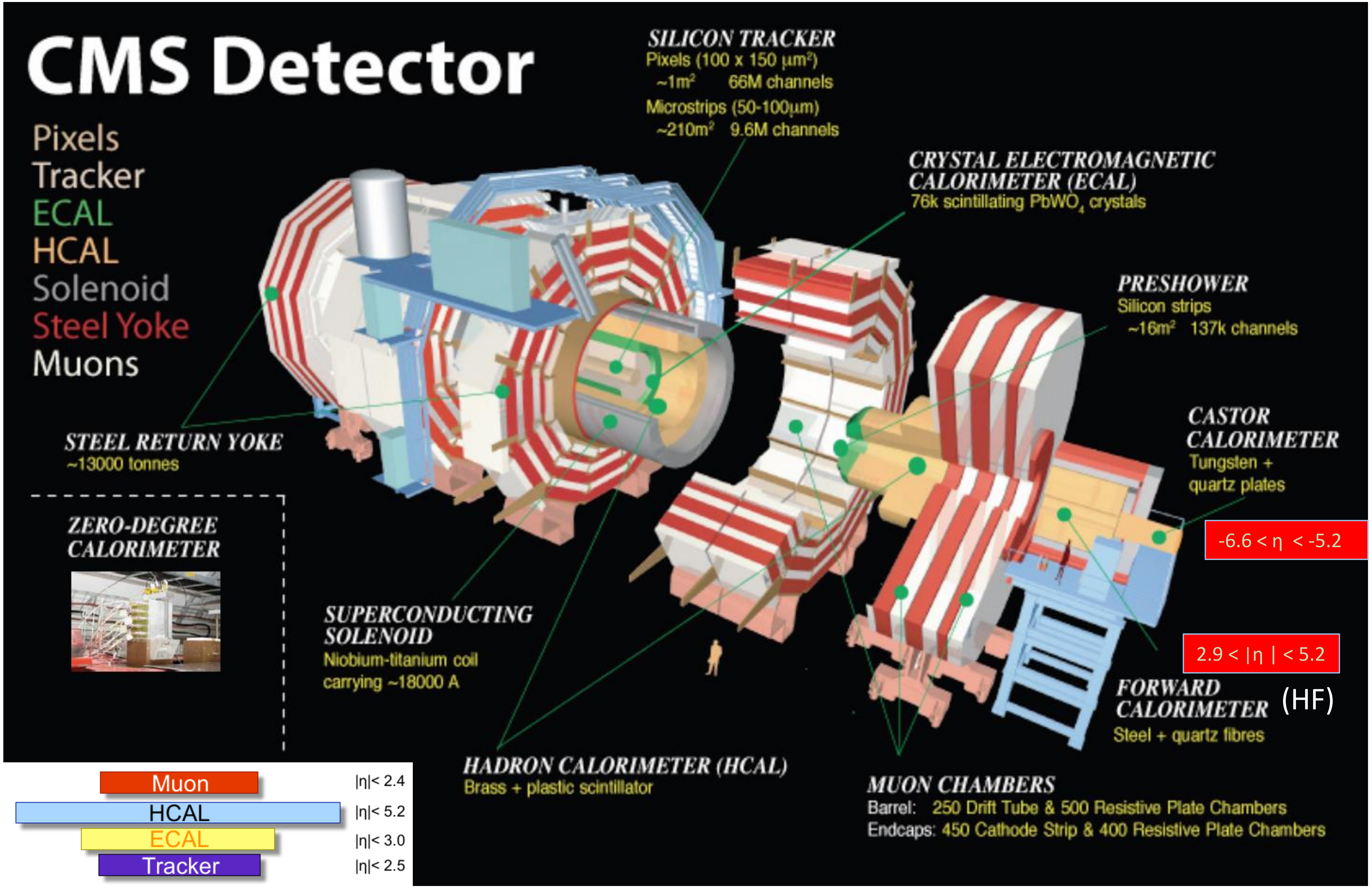
CMS Detector
Pixels
Tracker
ECAL
HCAL
Solenoid
Steel Yoke
Muons
SILICON TRACKER
Pixels (100 x 150 μm^2)
~1m^2 66M channels
Microstrips (50-100μm)
~210m^2 9.6M channels
CRYSTAL ELECTROMAGNETIC CALORIMETER (ECAL)
76k scintillating $PbWO_4$ crystals
PRESHOWER
Silicon strips
~16m^2 137k channels
CASTOR CALORIMETER
Tungsten + quartz plates
$-6.6 < \eta < -5.2$
$2.9 < |\eta| < 5.2$
FORWARD CALORIMETER (HF)
Steel + quartz fibres
STEEL RETURN YOKE
~13000 tonnes
ZERO-DEGREE CALORIMETER
SUPERCONDUCTING SOLENOID
Niobium-titanium coil carrying ~18000 A
HADRON CALORIMETER (HCAL)
Brass + plastic scintillator
MUON CHAMBERS
Barrel: 250 Drift Tube & 500 Resistive Plate Chambers
Endcaps: 450 Cathode Strip & 400 Resistive Plate Chambers
Muon $|\eta| < 2.4$
HCAL $|\eta| < 5.2$
ECAL $|\eta| < 3.0$
Tracker $|\eta| < 2.5$

Particle flow (PF) algorithm

The algorithm combines tracker (at |η|<2.5), calorimeter and muon detector information to assign all signals to one of 5 particle types:

1. **Muons**
2. **Electrons**
3. **Charged Hadrons**
4. **Neutral Hadrons**
5. **Photons**

- **Calorimeters signals associated with a track are removed and the energy is estimated from the track momentum**
- **Calorimeter energy is only used for the neutral hadrons and photons**

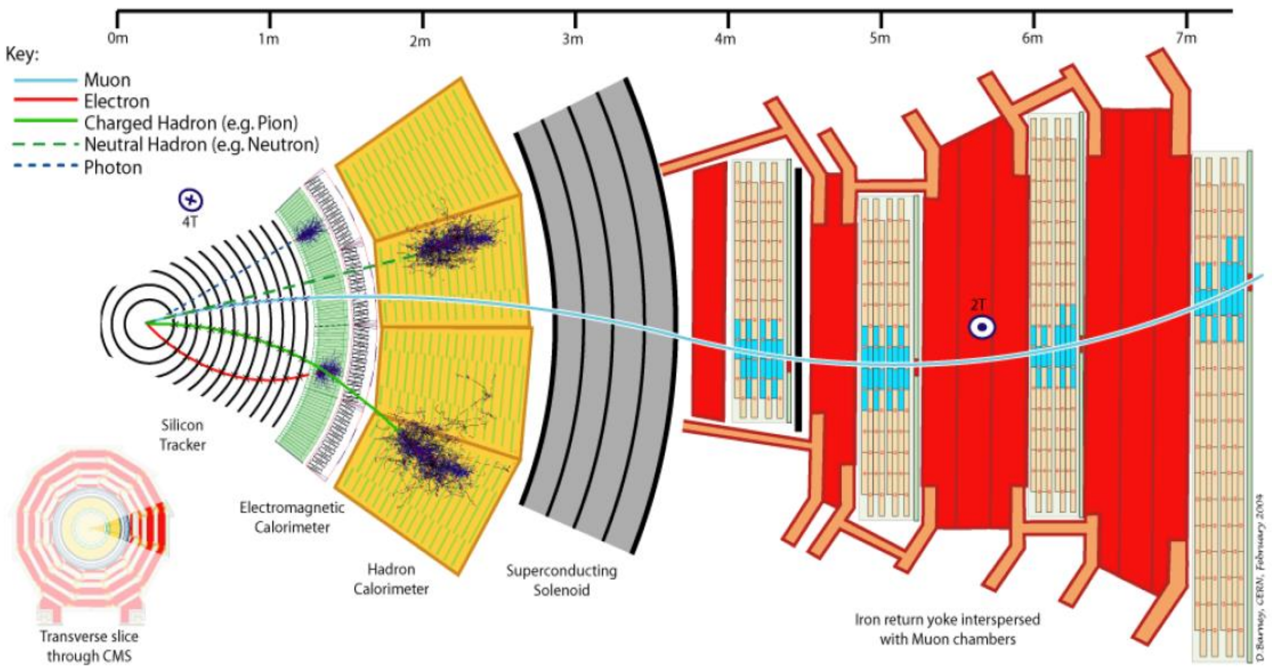

pp 7 TeV

PhysRevD.92.012003

Soft diffractive cross-sections

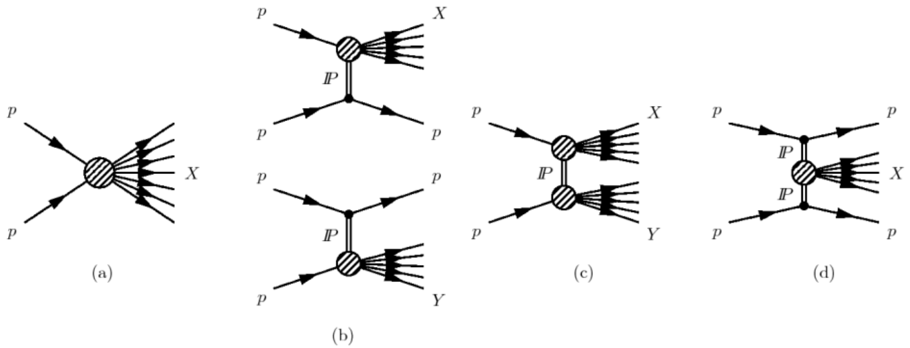

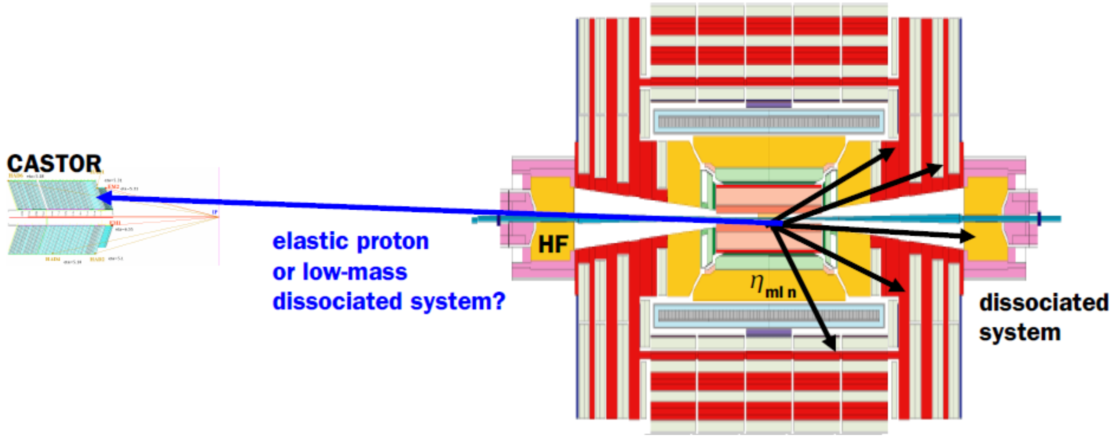

- Based on Particle Flow objects
- Single diffraction (SD) and double diffraction (DD) separated with CASTOR

Diffractive systems are two groups of particles on hadron level or PF objects on detector level separated by largest rapidity gap. Rapidity gap (RG) is interval in pseudorapidity devoid of activity (either on detector or hadron level).
SD and DD cross sections are measured as function of ζ.

✓ On detector level, ζ is measured as

$$\boxed{\xi = \frac{\sum(E^i + p_z^i)}{\sqrt{s}} \sim \frac{M_X^2}{s}}$$

✓ On hadron level, masses M_X and M_Y are calculated from full set of four-vectors in respective group of particles

ξ dependence

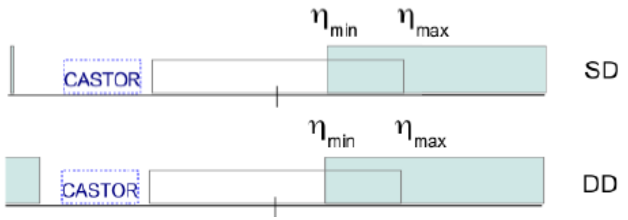

no CASTOR-tag (SD dominated)

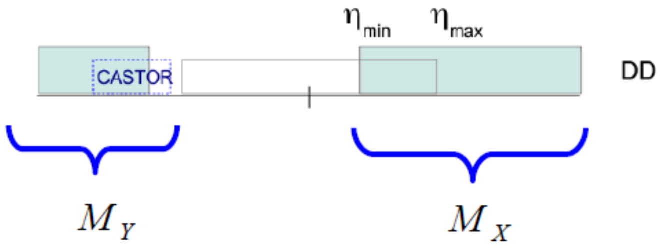

CASTOR-tag (DD dominated)

Single diffraction (SD) enriched

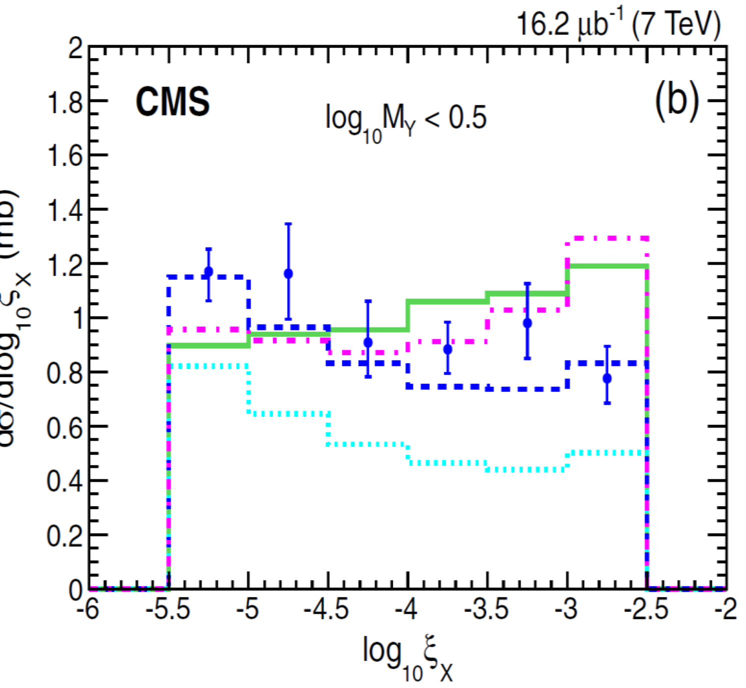

Double diffraction (DD) enriched

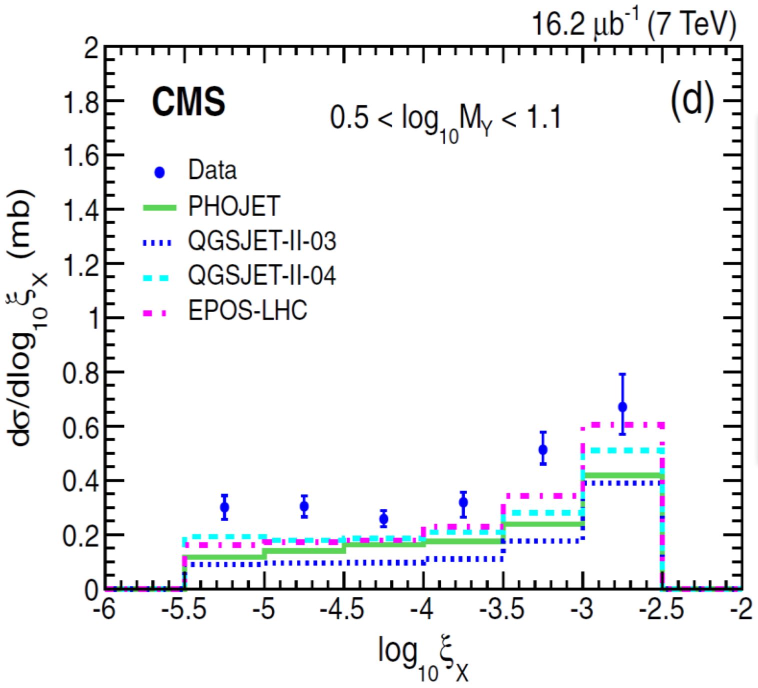

- For SD, EPOS-LHC is **close to data** (except last point), QGSJET-II-04 is **below data by factor ~2**.
- For DD both EPOS-LHC and QGSJET-II-04 are below data

Forward rapidity gaps

“Forward” rapidity gap implies that gap starts at most forward in used acceptance of detector pseudorapidity.

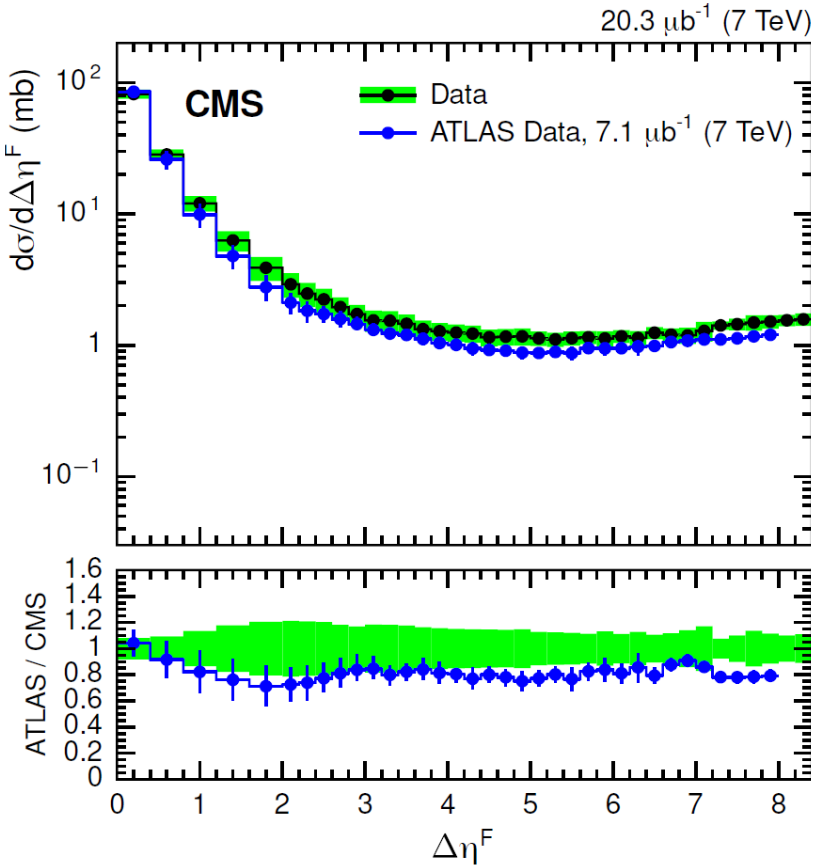

Good agreement of CMS with ATLAS

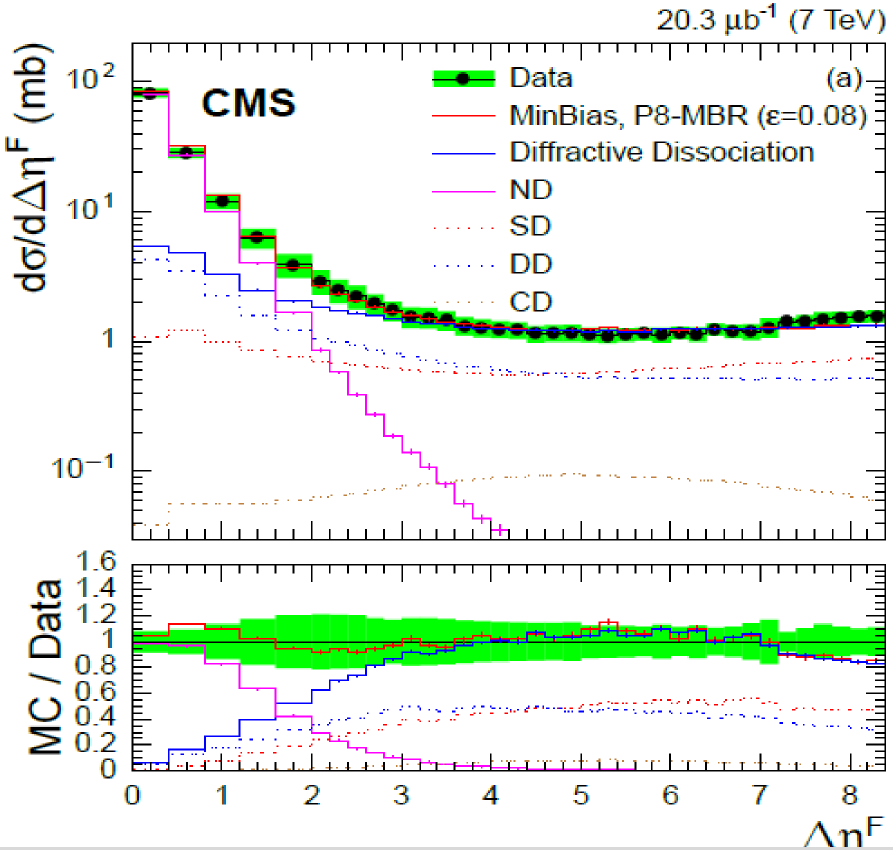

Large fraction of non-diffractive events can be suppressed by $\Delta\eta^F > 3$ cut.

pPb 8.16 TeV

New measurements (CMS-PAS-HIN-18-019)

In more detail

Previous mesurements

HELIOS, √s= 27 GeV Z. Phys. C 49 (1999) 355

DIFFRACTION DISSOCIATION OF NUCLEI IN 450 GeV/c PROTON-NUCLEUS COLLISIONS

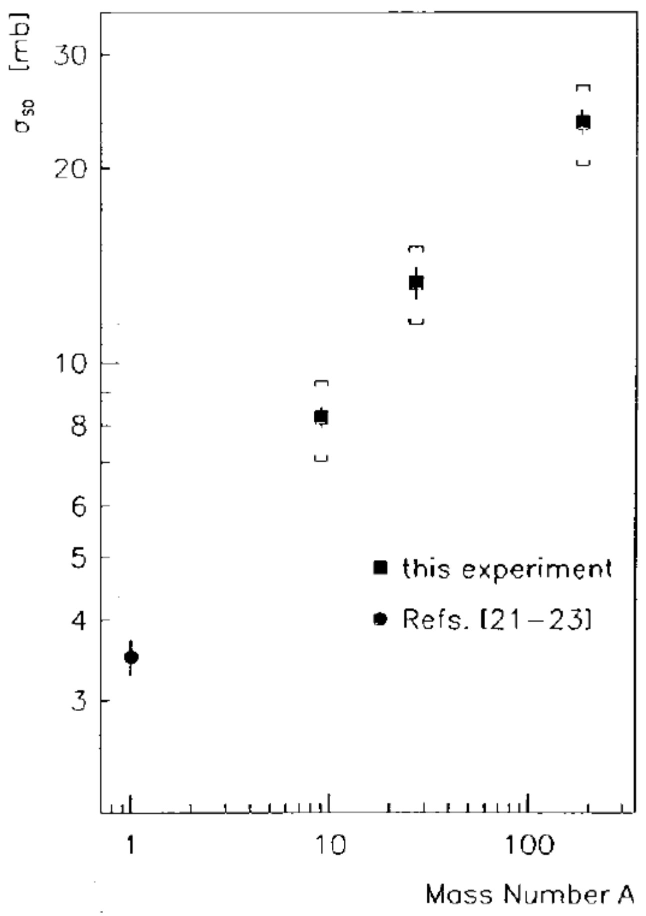

A-dependence

$\sigma=\sigma_0 A^{\alpha}$

$\alpha=0.35 \pm 0.02$ (stat.) $\pm$ 0.03 (syst.)

Data, event topology

Data: CMS, pPb $\sqrt{s_{NN}}$ = 8.16 TeV; 6.4μb^{-1}(2016).

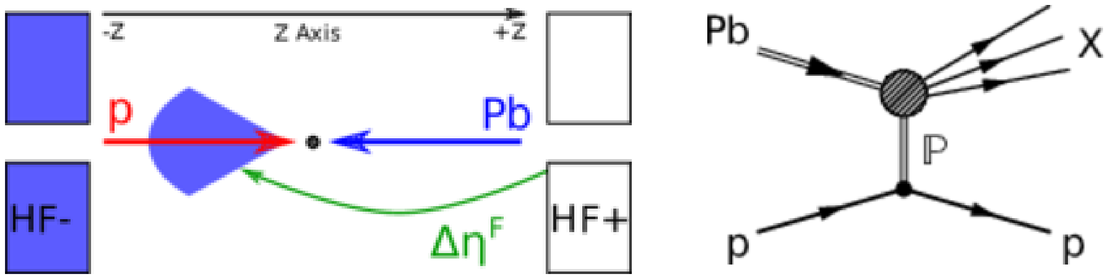

Lead dissociation

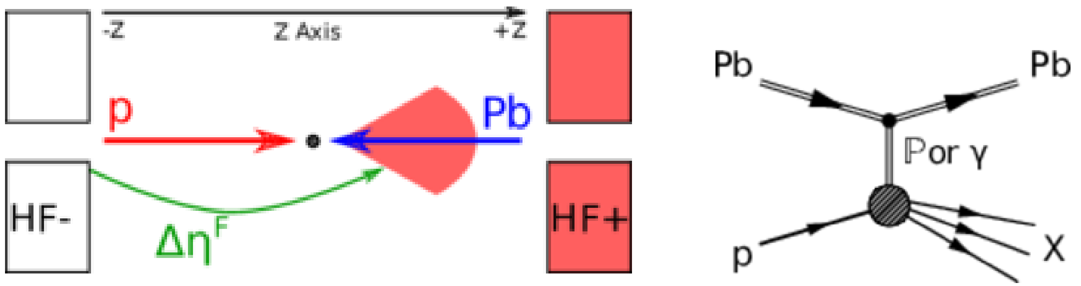

Proton dissociation

Measurements are done in two steps

- measurement of rapidity gap distribution in central part of detector at $-3<\eta<3$
- adding up HF calorimeters to acceptance at $-5.2<\eta<-3$, $3<\eta<5.2$

Two-step procedure is caused by different treatment of "emptiness" of η intervals in central detector and HF.

Monte Carlo

- EPOS-LHC: Gribov-Regge theory for the parton interactions, phenomenological implementation of gluon saturation.
- QGSJET II-04: Gribov-Regge theory for the parton interactions, gluon saturation via higher order pomeron-pomeron interactions.
- HIJING v2.1: Pythia-based, hard parton scatterings with perturbative QCD, soft interactions, string excitations.

Those generators do not include photon exchange processes.

Rapidity gaps in central detector

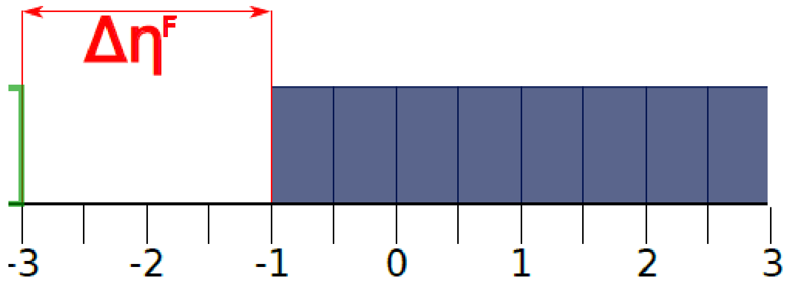

12 bins in pseudorapidity of size 0.5

- For $|\eta| < 2.5$:
  No track with $p_T > 200$ MeV
  Total energy of all PF objects < 6 GeV
- For $2.5 < |\eta| < 3.0$:
  Total energy of all PF hadronic objects < 13.4 GeV

Rapidity gap in central detector

Detector level

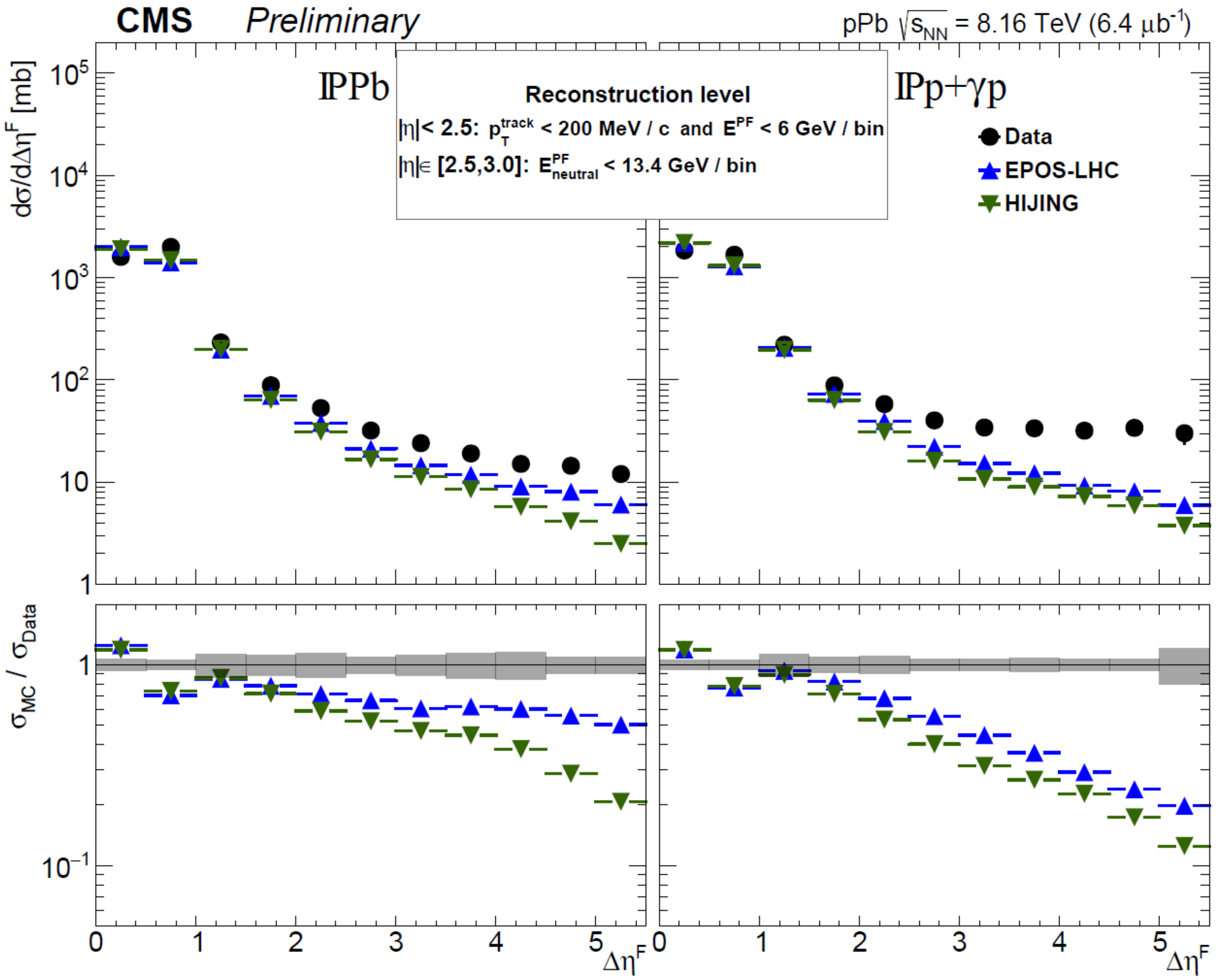

The Monte Carlo spectra are normalized to the total visible cross-section of the data.

- For both topologies, IPPb and IPp (IP stands for pomeron), MC are close to data at small $\Delta\eta^F$.
- At large $\Delta\eta^F$, for IPPb topology, i.e. dissociation of lead, data above EPOS-LHC by factor two and more above HIJING
- At large $\Delta\eta^F$, for IPp topology, i.e. dissociation of proton, data get much above MC due to contribution of γp events

Contribution of different processes

Stacked distributions

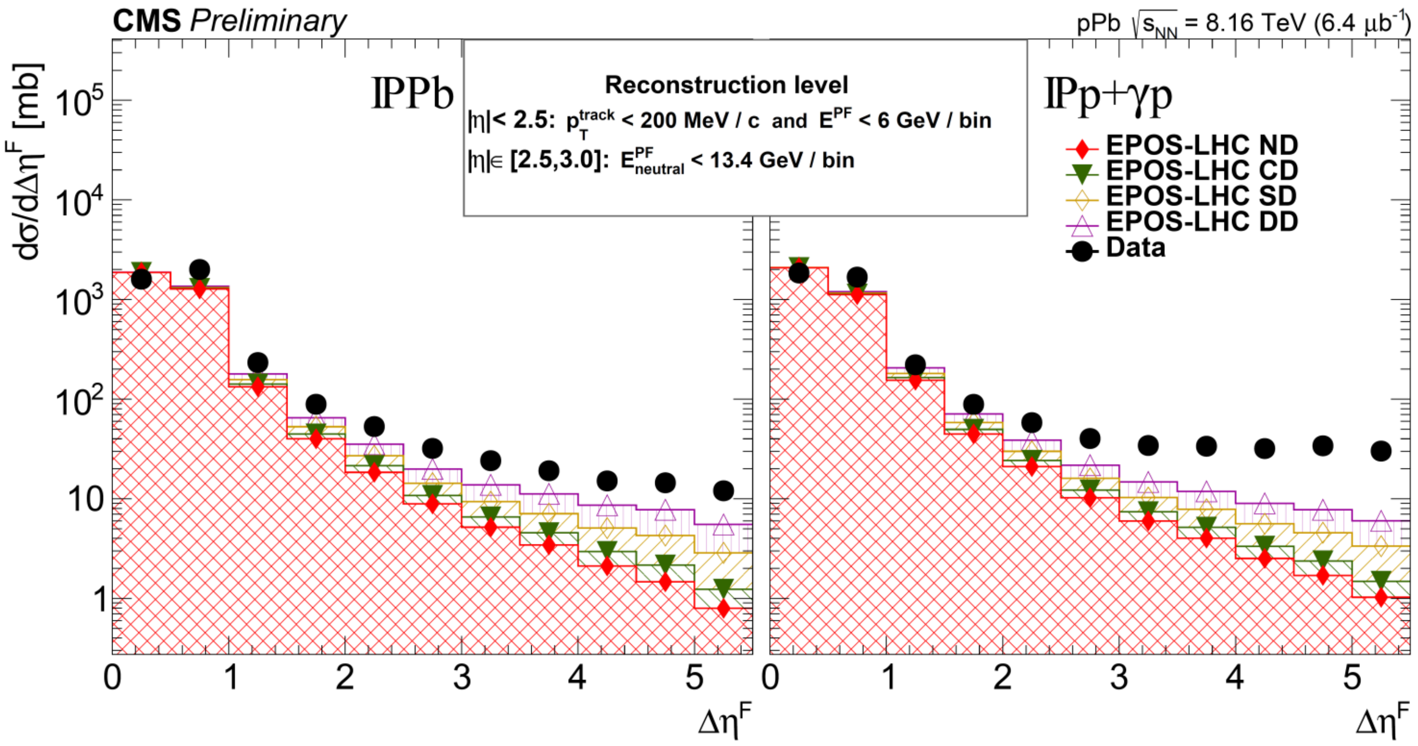

- At small $\Delta\eta^F$, non-diffractive processes dominate.
- Significant excess of diffraction over non-diffractive contribution appears only at large $\Delta\eta^F$.

Extension of acceptance with HF

HF calorimeters are placed at two sides of CMS at $-5.2 < \eta < -3$ and $3 < \eta < 5.2$. Each calorimeter contains 432 towers

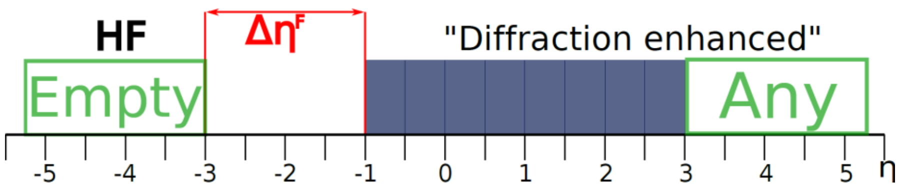

To extend rapidity gap size requirement of low activity in HF was added. That was done at detector level by cut on leading tower energy E_{max}<2.5 GeV. At hadron level, it was required that no particles of any energy enter HF. Efficiency correction was performed on data-only basis with use of no-collision events, in which leading tower energy distribution was fitted to analysed data at E_{max}<2.5 GeV. Purity correction was done with use of MC.

We present thus obtained results in same pseudorapidity bins as before. Since adding up HF allows to much enhance diffractive processes contribution these results are titled "**diffraction enhanced**". It is implied that to compare with e.g. pp results one should add $\Delta\eta$=2.2 to the presented $\Delta\eta^F$.

Unfolding to hadron level

Rapidity gap at the hadron level

- η=[-2.5,2.5] in bins of η=0.5
  - no charged particles with p_T > 200 MeV
  - total energy in the bin E < 6 GeV
- Edge bins 2.5<|η|<3

  total energy in the bin: E < 13.4 GeV
- HF acceptance

  no detectable particles

Unfolding is done with iterative Bayesian method

$$x_j^{ITER+1} = x_j^{ITER} \sum_i \frac{A_{ij}}{\varepsilon_j} \frac{y_i^{data}}{\sum_k A_{ik} x_k^{ITER}}$$

Unfolded diffractive enhanced spectra

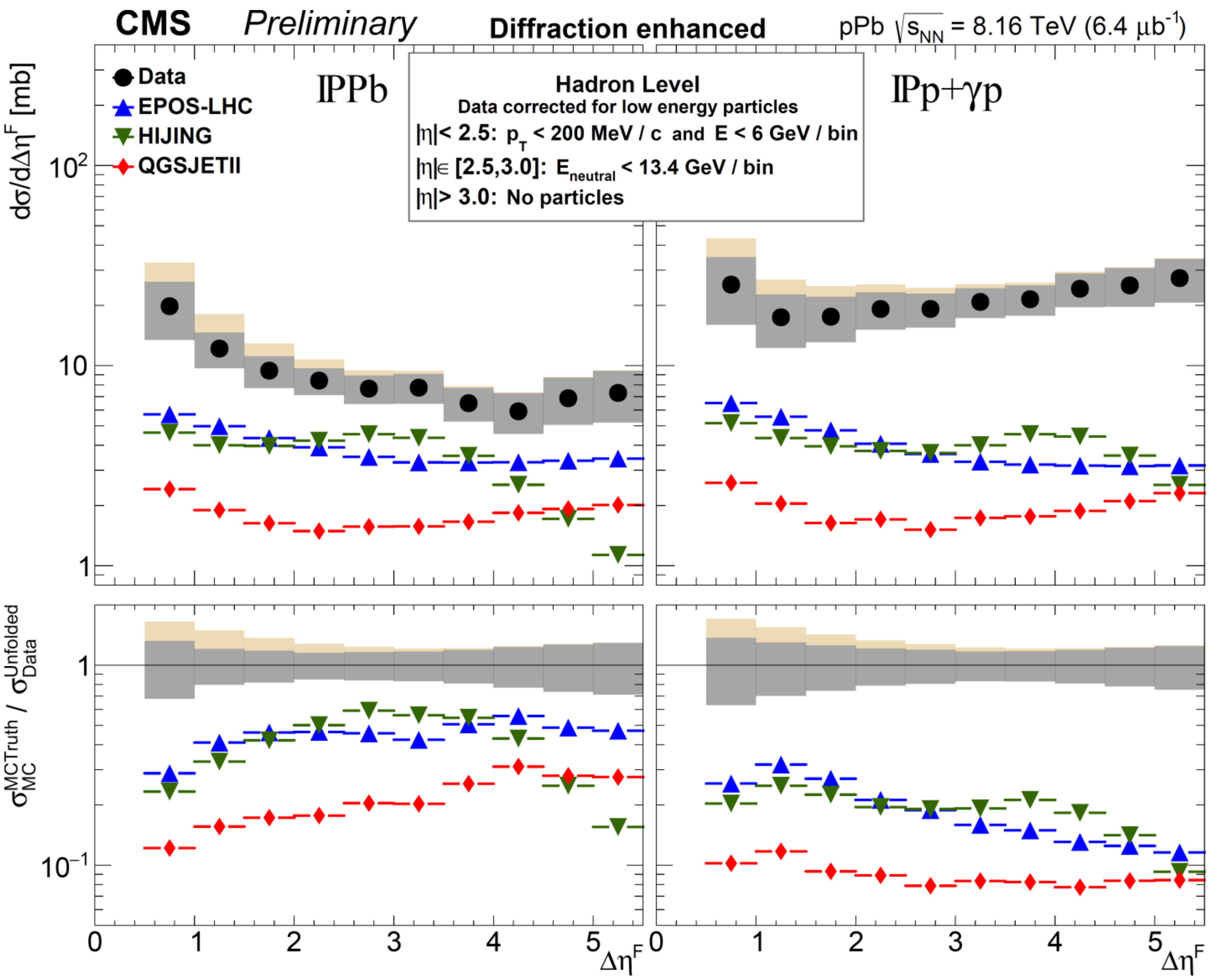

For **IPPb** topology case (γ-exchange contribution negligible):

- At large $\Delta\eta^F$, where contribution of non-diffractive events is small,EPOS-LHC is about a factor of 2 and QGSJETII-04 is about a factor of 4 below data.
- HIJING demonstrates sharp decline at large $\Delta\eta^F$, which is a consequence of deficit of low-mass diffraction in the generator.
- Some rise of spectrum at large $\Delta\eta^F$ should be noted in data as well as in cosmic ray MC

For **IPp** topology, all generators are significantly below data. This suggests very strong contribution from γp events non-simulated in considered generators.

- QGSJETII-04 is much below two other generators.
- EPOS-LHC and QGSJETII-04 are different in shape, with QGSJETII-04 being closer in shape to data. That could point to insufficient contribution of low-mass diffraction in EPOS-LHC.

Contribution of different processes

Stacked distributions for two generators

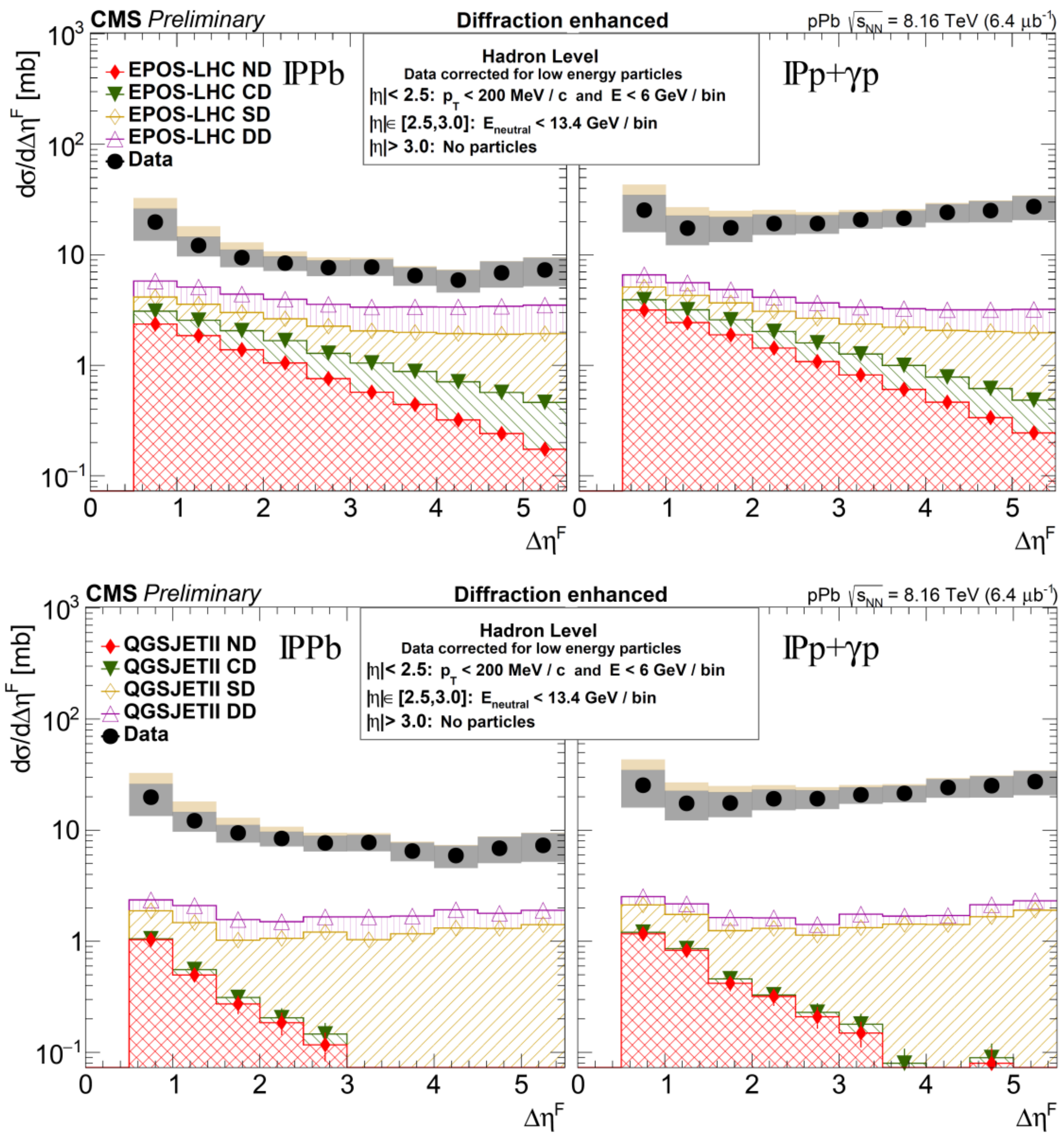

- Non-diffraction noticeably contributes only at smallest gaps, resulting in rise of total distribution.
- This contribution is larger in EPOS-LHC, moving MC predictions closer to data than that of QGSJETII-04 and providing difference in shape of distributions between two generators.
- Cross-section of diffraction in QGSJETII-04 is about two times smaller than in EPOS-LHC, which is most certain at large $\Delta\eta^F$, where non-diffractive contribution is small.
- If we compare cross-sections of target diffraction (IIPPb) at $\Delta\eta^F > 4$ where contribution of non-diffractive events is negligible with CMS pp data at corresponding $\Delta\eta^F > 6$ we obtain ratio σ_{pPb}/σ_{pp} ~6 which perfectly fits A-dependence $A^{0.35}$ demonstrated in HELIOS experiment.

Summary

- **pp 7 TeV :**
  - EPOS-LHC is **close to data**.
  - QGSJETII-04 is about a **factor of 2 below data.**
- **pPb 8 TeV :**

  For **IPPb** topology where γ-exchange contribution is negligible:
  - **At large $\Delta\eta^F$, comparison with corresponding cross-sections of pp measurements results in A-dependence which perfectly fits $A^{0.35}$ dependence obtained in HELIOS experiment.**
  - At large $\Delta\eta^F$, cross-sections of EPOS-LHC is about **a factor of 2 below data**.
  - At large $\Delta\eta^F$, cross-sections of QGSJETII-04 is about a **factor of 4 below data**

  For **IPp** topology, all generators are much more below data. This suggests very strong contribution from γp events non-simulated in considered generators:
  - QGSJETII-04 is much below two other generators.
  - EPOS-LHC and QGSJETII-04 are different in shape, QGSJETII-04 being closer in shape to data.
- Relative difference between QGSJETII-04 and EPOS-LHC is the same for **pPb** and **pp**, with QGSJETII-04 giving lower cross-sections than EPOS-LHC at large $\Delta\eta^F$ by about factor of two, but **both MC moved down from data** by about factor of two for **IPPb** topology in **pPb** relative to **pp**. That points to **difficulties with describing nuclear effects** in generators.